

# Synchronization analysis for stochastic multi-layer networks: Event-based impulsive control with predefined impulsive intervals

Hengyu Liu<sup>a</sup>, Jiarong Li<sup>a, 1</sup>, Haijun Jiang<sup>b</sup>, Jinling Wang<sup>c</sup>, Cheng Hu<sup>a</sup>

<sup>a</sup>College of Mathematics and System Science, Xinjiang University, Urumqi, 830017, Xinjiang, China liuhymath@163.com; ljrmath@163.com; wacheng2003@163.com

<sup>b</sup>College of Mathematics and Statistics, Yili Normal University, Yining, 835000, Xinjiang, China jianghaijunxju@163.com

<sup>c</sup> School of Science, Jimei University, Xiamen, 361021, China jinling0803@126.com

Received: June 28, 2024 / Revised: September 26, 2025 / Published online: October 20, 2025

**Abstract.** This article explores the novel approach to addressing the intra/inter-layer synchronization challenges in stochastic multi-layer networks (SMLNs). First, considering the influence of time delay in control, an event-triggered delayed impulsive control (ETDIC) strategy is developed, where the impulsive instant is determined by the predesigned event-triggered mechanism. Moreover, by introducing piecewise auxiliary functions, it effectively excludes Zeno behavior within the ETDIC framework. The study then derives sufficient conditions for ensuring intra- and inter-layer synchronization, leveraging the Lyapunov method and rigorous mathematical analysis. Finally, theoretical results are validated through numerical simulations.

**Keywords:** stochastic multi-layer networks, intra-layer synchronization, inter-layer synchronization, event-triggered delayed impulsive control.

#### 1 Introduction

In recent years, multi-layer networks (MLNs) have attracted extensive scholarly attention due to their broad applications in power systems, biology, and related fields [13, 16, 30].

<sup>&</sup>lt;sup>1</sup>This work was supported by the Natural Science Foundation of Xinjiang Uygur Autonomous Region (grant No. 2025D01C32) and Key Project of Natural Science Foundation of Xinjiang Uygur Autonomous Region (grant No. 2024D01D04), the National Natural Science Foundation of People's Republic of China (grant No. 62163035), and the Special Project for Local Science and Technology Development Guided by the Central Government (grant No. ZYYD2022A05).

<sup>© 2025</sup> The Author(s). Published by Vilnius University Press

This is an Open Access article distributed under the terms of the Creative Commons Attribution Licence, which permits unrestricted use, distribution, and reproduction in any medium, provided the original author and source are credited.

Synchronization, a critical property of MLNs, plays a vital role in parameter identification, image processing, and secure communication. Significant research has addressed synchronization in MLNs [1, 26], which can be categorized into three types: complete synchronization [4, 29], intra-layer synchronization [10, 23], and inter-layer synchronization [14, 15]. Intra-layer synchronization coordinates nodes with heterogeneous states within individual layers, while inter-layer synchronization governs cross-layer information transmission and communication, critically influencing network-wide learning and parameter updating processes.

Previous synchronization studies often presume noise-free MLNs models, an assumption inconsistent with real-world conditions. Stochastic disturbances ubiquitous in network environments due to unpredictable events significantly impair information transmission in multi-layer networks. Examples include social network turbulence, random epidemics in biological systems, and stochastic resonances in chemical processes [7, 12, 22]. While functionally characterizing such interference remains challenging, substantial research now addresses stochastic effects in MLNs [17, 26]. For instance, Zhang et al. used graph theory to analyze the topology identification of SMLNs [26], while Ren et al. investigated exponential synchronization of complex-valued SMLNs through discontinuous control [17]. This underscores the importance and intrigue of analyzing SMLNs in depth.

Networks typically lack spontaneous synchronization, necessitating efficient control mechanisms to steer states toward desired trajectories. Advanced strategies proposed to address this include event-triggered control [27], pinning control [19], intermittent control [11], sampled-data control [28], impulsive control [3], and adaptive control [6]. Among these, impulsive control distinguishes itself by its interference robustness, implementation simplicity, and cost-effectiveness, attracting growing research interest. As a discrete-time strategy, the impulsive controller activates only at specific instants to induce instantaneous state jumps. Significant advances in impulsive control have been documented [2, 9, 18], including Shi et al.'s work on quasi-synchronization in multi-layer neural networks [18] and Ling et al.'s analysis of exponential synchronization in delayed neural networks [9].

However, existing studies overlook the time delays inherent in pulse generation during impulsive control. Constraints in information transmission speed and process complexity cause such delays to severely degrade system response and performance. For instance, in residential smart lighting systems, activating a fixture via voice command or mobile app initiates a pulse signal. Inherent communication or processing delays then cause latency between pulse triggering and action execution. Consequently, incorporating time-delay effects, precisely delayed impulsive control is essential when designing impulsive control strategies.

While numerous articles have explored delayed impulsive control [8,31], the majority of this work has focused on time-triggered impulsive control. This approach operates within predefined time intervals, restricting events or actions to specific temporal boundaries. Missing an event necessitates waiting for the next scheduled instance, highlighting the inherent conservatism of time-triggered mechanisms. To overcome these constraints, ETDIC was proposed [21, 24]. Specifically, Wang et al. investigated synchronization

problems for complex networks under ETDIC, demonstrating its ability to trigger control actions solely based on system state deviations or the fulfillment of specific conditions [21]. In contrast to time-triggered impulsive control, ETDIC optimizes the utilization of computational and communication resources, enhancing system real-time capabilities and overall performance. Yang et al. further analyzed the synchronization challenges of stochastic complex networks under ETDIC, demonstrating enhanced resilience against external disturbances and noise [24].

Based on the above analysis and observation, we study intra/inter-layer synchronization problem of SMLNs under ETDIC. The main contributions of this paper are as follows:

- (i) From the perspective of model, we introduce a novel complex network model that incorporates both intra- and inter-layer couplings, driven by Brownian motion.
- (ii) From the perspective of control methods, two new delayed impulsive control schemes based on Lyapunov functions are proposed, where impulsive instants are jointly determined by a preset event-triggered mechanism and a predefined impulsive interval.
- (iii) From the perspective of content, by leveraging auxiliary functions to eliminate the influence of random disturbances we cleverly eliminate Zeno behavior. Some new intra/inter-layer synchronization criteria are obtained using stochastic analysis technique and Lyapunov method.

The subsequent sections of this paper are structured as follows: Section 2 provides an overview of SMLNs and introduces the necessary foundational concepts. In Section 3, sufficient conditions are presented for SMLNs to prevent Zeno behavior, along with discussions on intra-layer synchronization and inter-layer synchronization. Section 4 demonstrates the analytical process through numerical simulations. Finally, Section 5 elaborates on the conclusions drawn from the study.

**Notations.**  $\mathbb{R}$  and  $\mathbb{R}^+$  are the sets of real numbers and positive real numbers, respectively.  $\mathbb{R}^n$  denotes the n-dimensional Euclidean space.  $\mathbb{R}^{n \times n}$  is the sets of  $n \times n$ -dimensional matrices.  $\|\cdot\|$  stands for the Euclidean norm of a vector or matrix. Let  $I_n$  represent the n-dimensional identity matrix.  $M^{\mathrm{T}}$  is the transpose of matrix M.  $\mathrm{trace}(\cdot)$  denotes the trace operator of the matrix.  $\lambda_{\mathrm{max}}(\cdot)$  represents the largest eigenvalue of the matrix.  $\otimes$  is the Kronecker product. \* denotes the symmetric term in a symmetric matrix. Denote  $(\Omega, \mathcal{F}, \{\mathcal{F}_t\}_{t\geqslant 0}, \mathbf{P})$  as a complete probability space, where the filtration  $\{\mathcal{F}_t\}_{t\geqslant 0}$  satisfies the usual conditions. Define  $\mathcal{L}$  as the differential operator acting on Lyapunov function V(t).

## 2 Preliminaries and problem description

#### 2.1 Algebraic graph theory

Consider a multi-layer undirected graph  $\mathcal{G}^r = (\mathcal{V}, \mathcal{E}^r, \mathcal{A}^r)$ , where  $\mathcal{V} = \{v_1, \dots, v_N\}$  denotes the vertex set, and  $\mathcal{E}^r \subseteq \mathcal{V} \times \mathcal{V}$  indicates the undirected edge set of rth layer.

 $\mathcal{A}^r=(a^r_{ij})_{N\times N}\in\mathbb{R}^{N\times N} \text{ represents the adjacency matrix of } \mathcal{G}^r, \text{ where } a^r_{ij}=a^r_{ji}=1, \text{ if there is a link between nodes } i \text{ and } j \text{ in } r\text{th layer, otherwise, } a^r_{ij}=a^r_{ji}=0. \text{ The degree matrix of } r\text{th layer is defined by } \mathcal{O}^r=\operatorname{diag}(o^r_1,o^r_2,\ldots,o^r_n), \, o^r_i=\sum_{j=1}^N a^r_{ij}. \text{ Similarly, } D=(d_{rk})_{M\times M}\in\mathbb{R}^{M\times M}, \text{ where } d_{rk}=-1, \text{ if there is a one-to-one connection between the nodes in the } r\text{th layer and the } k\text{th layer, otherwise, } d_{rk}=0. \text{ Furthermore, let } d_{rr}=-\sum_{k=1,\,k\neq r}^M d_{rk}.$ 

## 2.2 Problem description

The model of SMLNs is composed of N nodes of M layer, which is depicted by

$$dx_{i}^{r}(t) = \left[ -Cx_{i}^{r}(t) + Bf(x_{i}^{r}(t)) - \alpha \sum_{j=1}^{N} l_{ij}^{r} Hx_{j}^{r}(t) - \beta \sum_{k=1}^{M} d_{rk} \Gamma x_{i}^{k}(t) + u_{i}^{r}(t) \right] dt + g(t, x_{i}^{r}(t)) dw(t),$$
(1)

where  $i=1,2,\ldots,N,\,r=1,2,\ldots,M,\,x_i^r=(x_{i1}^r,x_{i2}^r,\ldots,x_{in}^r)^{\rm T}\in\mathbb{R}^n$  indicates the state vector of the ith node in the kth layer.  $C={\rm diag}(c_1,c_2,\ldots,c_n)$  is a positive-definite diagonal matrix.  $B\in\mathbb{R}^{n\times n}$  is the connection weight matrix.  $f(\cdot)$  is the nonlinear function. Constants  $\alpha$  and  $\beta$  are the intra-layer and inter-layer coupling strengths, respectively.  $H\in\mathbb{R}^{n\times n}$  and  $\Gamma\in\mathbb{R}^{n\times n}$  are the candidates for inner coupling symmetric matrices that describe the coupling between state components of nodes. The Laplacian matrix of rth layer  $L^r=(l_{ij}^r)_{N\times N}\in\mathbb{R}^{N\times N}$  is defined as  $L^r=\mathcal{O}^r-\mathcal{A}^r.$   $u_i^r(t)$  is the control input of the ith node in the ith layer to be designed. i0 denotes the noise intensity function. i1 i2 a standard Brownian motion defined on i3. i4 i5 denotes the noise intensity function.

**Remark 1.** Previous studies [6, 11, 19, 28] did not focus on the inter-layer coupling of SMLNs itself, whereas the nonlinear inter-layer coupling of SMLNs was explored in [4]. Although [22] addresses inter-layer coupling in MLNs, it assumes the inter-layer internal coupling matrix is identical to the intra-layer internal coupling matrix. Building upon insights from [4, 22], the SMLNs model proposed in this paper incorporates a distinct inter-layer coupling mechanism, increasing the model's versatility.

Remark 2. Complex industrial systems, such as smart grids and biological neural networks, commonly exhibit stochastic disturbances, multi-layer coupling structures, and control delays that severely constrain coordination efficiency. Resolving intra-layer synchronization ensures behavioral consistency among homogeneous functional units (e.g., voltage synchronization in generator clusters within power grids), thereby preventing localized instabilities from triggering cascading failures. Achieving inter-layer synchronization guarantees cross-layer coordination efficiency (e.g., dynamic power matching between transmission and distribution grids), enhancing overall system resilience. The ETDIC framework has been validated in critical domains including smart city infrastructure and industrial internet, providing theoretical foundations and practical paradigms for constructing interference-resistant, cost-effective coordinated control systems.

**Lemma 1.** (See [5].) For any positive-definite matrix  $\Pi \in \mathbb{R}^{n \times n}$  and  $x, y \in \mathbb{R}^n$ , the following inequality holds:

$$2x^{\mathrm{T}}y \leqslant x^{\mathrm{T}}\Pi x + y^{\mathrm{T}}\Pi^{-1}y.$$

Lemma 2 [Schur complement]. (See [32].) The linear matrix inequality

$$\begin{bmatrix} S_{11} & S_{12} \\ S_{12}^{\rm T} & S_{22} \end{bmatrix} < 0$$

is equivalent to any of the following conditions:

- (i)  $S_{22} < 0$  and  $S_{11} S_{12}S_{22}^{-1}S_{12}^{T} < 0$ ,
- (ii)  $S_{11} < 0$  and  $S_{22} S_{12}^{\mathrm{T}} S_{11}^{-2} S_{12} < 0$ .

Here  $S_{11}^{T} = S_{11}$  and  $S_{22}^{T} = S_{22}$ .

**Assumption 1.** . For any  $x, y \in \mathbb{R}^n$ , there exists a positive constant q such that nonlinear function  $f(\cdot)$  satisfies

$$||f(x) - f(y)|| \le q||x - y||.$$

**Assumption 2.** For any  $x, y \in \mathbb{R}^n$ , there exists a positive constant  $\mu$  such that

$$\operatorname{trace}((g(t,x)-g(t,y))^{\mathrm{T}}(g(t,x)-g(t,y))) \leqslant \mu(x-y)^{\mathrm{T}}(x-y).$$

## 3 Main results

## 3.1 Intra-layer synchronization

In this section, intra-layer synchronization is researched. Consider the tracking target  $s^r(t)$  of all nodes in the rth layer of network (1) as follows:

$$ds^{r}(t) = \left[ -Cs^{r}(t) + Bf(s^{r}(t)) - \beta \sum_{k=1}^{M} d_{rk} \Gamma s^{k}(t) \right] dt + g(t, s^{r}(t)) dw(t).$$
 (2)

Define synchronization error  $e_i^r(t) = x_i^r(t) - s^r(t)$ . From networks (1) and (2) the synchronization error system is

$$de_{i}^{r}(t) = \left[ -Ce_{i}^{r}(t) + Bf(e_{i}^{r}(t)) - \alpha \sum_{j=1}^{N} l_{ij}^{r} He_{j}^{r}(t) - \beta \sum_{k=1}^{M} d_{rk} \Gamma e_{i}^{k}(t) + u_{i}^{r}(t) \right] dt + g(t, e_{i}^{r}(t)) dw(t),$$
(3)

where  $f(e_i^r(\cdot)) = f(x_i^r(\cdot)) - f(s^r(\cdot)), \ g(e_i^r(\cdot)) = g(x_i^r(\cdot)) - g(s^r(\cdot)).$ 

For achieving intra-layer synchronization of networks (1), the ETDIC scheme is characterized as

$$u_i^r(t) = \sum_{\kappa=1}^{\infty} \left( K e_i^r(t - \tau_\kappa) - e_i^r(t) \right) \delta(t - t_\kappa^r), \quad \kappa \in \mathbb{Z}^+, \tag{4}$$

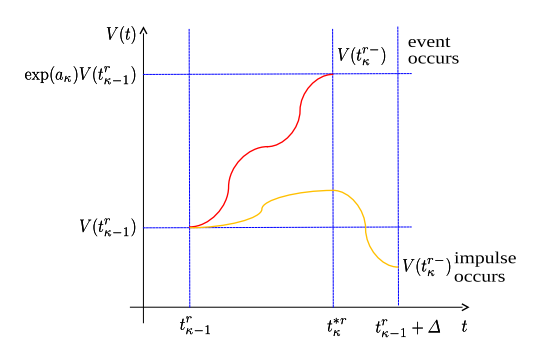


Figure 1. Triggered principle of event-triggered mechanism (5).

where matrix  $K \in \mathbb{R}^{n \times n}$  is impulsive control gain, and  $\delta(\cdot)$  is the Dirac delta function.  $\tau_{\kappa}$  is the time delay in impulsive control satisfying  $\tau_{\kappa} \in [0, \tau]$ .

$$t_{\kappa}^{r} = \min\{t_{\kappa}^{*r}, t_{\kappa-1}^{r} + \Delta\},\tag{5}$$

$$t_{\kappa}^{*r} = \inf \left\{ t \geqslant t_{\kappa-1}^r \colon \mathcal{E}V^r(t) \geqslant \exp(a_{\kappa})\mathcal{E}V^r(t_{\kappa-1}^r) \right\},\tag{6}$$

where  $\mathcal{E}V^r(t) = \mathcal{E}\sum_{i=1}^N (e_i^r(t))^{\mathrm{T}} e_i^r(t) = \mathcal{E}(e^r(t))^{\mathrm{T}} e^r(t)$ ,  $t_\kappa^r$  denotes the  $\kappa$ th impulsive instant of all node in the rth layer, positive parameter  $\Delta$  represents the predefined impulsive interval, supposing that  $\Delta \geqslant \tau$ ,  $a_\kappa$  satisfying  $\sum_{i=1}^\kappa a_i \to \infty$  as  $\kappa \to \infty$ .

**Remark 3.** The design of ETM (6) is mainly based on the Lyapunov function of the system (usually used to describe the energy state of the system). The event will only be triggered when the energy  $V^r(t)$  of the system exceeds the set energy threshold  $\exp(a_\kappa) \times V^r(t_{\kappa-1}^r)$ . This on-demand triggering method not only accelerates the convergence speed of the system but also reduces resource waste and improves resource utilization efficiency.

**Remark 4.** In event-triggered control research, it is customary to demand a positive time interval between adjacent triggering events to prevent the Zeno phenomenon. To better comprehend ETDIC (4) with (5), we present an illustration in Fig. 1. As depicted, if event (6) is triggered at  $t_{\kappa}^{*r}$  within the time interval  $[t_{\kappa-1}^r, t_{\kappa-1}^r + \Delta)$ , the impulse occurs at  $t_{\kappa}^{*r}$ . If event (6) is not triggered within the interval  $[t_{\kappa-1}^r, t_{\kappa-1}^r + \Delta)$ , the impulse arises at  $t_{\kappa-1}^r + \Delta$ .

**Remark 5.** The ETDIC (4) with (5) introduces a crucial enhancement over traditional event-triggered impulsive controllers by incorporating considerations for time delays during pulse generation. To demonstrate its practicality, envision a scenario with a smart lighting and outlet system for residential applications. When a user activates a light or socket via voice command or mobile app, the system generates a pulse signal. However, inherent network latency or device response times introduce delays between the triggering pulse and the actual execution of the action. When a user initiates a light switch through a mobile app, it may take several milliseconds or more for the system to receive and process the command due to network latency or communication issues. Despite the widespread adoption of event-triggered control strategies, such delays significantly

impact system response speed and performance. Our controller addresses this challenge by accounting for these delays, ensuring optimized system performance and enhanced user experience in practical applications.

Remark 6. The fundamental distinction between ETIC and ETIC with predefined impulsive intervals (ETIC-PII) lies in their triggering mechanisms and resulting pulse characteristics, ETPC operates purely event-driven: it continuously monitors a triggering condition and instantly applies a pulse at any arbitrary continuous time once the condition is met. This results in completely unpredictable pulse timing and highly variable inter-pulse intervals, dictated solely by system dynamics and the trigger threshold, with no occurrence of "void pulses". However, implementation typically requires complex continuous or highfrequency monitoring. Conversely, ETIC-PII employs a hybrid mechanism: it checks the triggering condition at fixed, predetermined time points, applying a pulse only at these scheduled times if the condition is satisfied (otherwise, generating a "void pulse" or "skip"). Consequently, pulses occur exclusively at predefined discrete instants with actual inter-pulse intervals being integer multiples of the fixed sampling period  $\Delta$  (enabled by skips), thereby maintaining a highly predictable temporal framework. This periodic sampling mechanism generally entails lower implementation complexity. In summary, ETPC seeks to maximize resource efficiency by minimizing total pulses at any time, while EBPC-PPI focuses on reducing unnecessary pulse executions within a fixed, predictable temporal structure.

Remark 7. While purely ETDIC theoretically offers the potential for maximal resource efficiency, ETIC-PII proves more appealing for the particular yet important application scenario of intra/inter-layer synchronization analysis. This advantage stems from the distinct benefits offered by its fixed-time framework: analytical tractability, enhanced coordination, predictable timing, and efficient resource scheduling. ETIC-PII effectively combines the resource-saving merits of event triggering with the temporal structure and predictability of time-triggered approaches. Consequently, it provides a more powerful and practical tool for the theoretical analysis and design of complex network synchronization problems. Its core strength lies in transforming the highly complex and challenging problem of asynchronous event-driven synchronization into a framework that can be modeled and analyzed on a regular time grid.

**Definition 1.** Networks (1) and (2) are said to achieve intra-layer synchronization under ETDIC (4) with (5) if  $\lim_{t\to\infty} \|x_i^r(t) - s^r(t)\| = 0$ , i = 1, 2, ..., N, r = 1, 2, ..., M.

Thus, combined with controller (4) with (5), error system (3) can be written as

$$de_{i}^{r}(t) = \left[ -Ce_{i}^{r}(t) + Bf(e_{i}^{r}(t)) - \alpha \sum_{j=1}^{N} l_{ij}^{r} He_{j}^{r}(t) - \beta \sum_{k=1}^{M} d_{rk} \Gamma e_{i}^{k}(t) \right] dt + g(t, e_{i}^{r}(t)) dw(t), \quad t \neq t_{\kappa}^{r},$$

$$e_{i}^{r}(t) = Ke_{i}^{r}(t^{-} - \tau_{\kappa}), \quad t = t_{\kappa}^{r},$$
(7)

where  $e(t^+)=e(t)$ , i.e., the solutions of system (7) are right-continuous at each discrete instant  $t^r_\kappa$ .

**Theorem 1.** Assume that there exist positive constants  $\sigma_1$  and  $a_{\kappa}$  satisfying  $a_{\kappa} \ge (1 + \sigma_1)\tau$  for all  $\kappa \in Z^+$  and a locally Lipschitz function  $V : \mathbb{R}^n \to \mathbb{R}^+$  satisfying

$$\mathcal{ELV}^r(t) \leqslant \sigma_1 \mathcal{EV}^r(t), \quad t \in [t_{\kappa-1}^r, t_{\kappa}^r).$$
 (8)

Then system (1) can avoid Zeno behavior under event-triggered mechanism (5). Moreover, the impulse time sequence  $\{t_{\kappa}^{r}\}$  satisfies

$$t_{\kappa}^r - t_{\kappa-1}^r \geqslant \min \left\{ \frac{a_{\kappa}}{1 + \sigma_1}, \Delta \right\} \quad \forall \kappa \in \mathbb{Z}^+.$$

*Proof.* Based on the definition of the event-triggered mechanism (5), it can be derived that the impulses will occur infinitely, so one can assume that the impulsive instants are  $t_1^r < t_2^r < \cdots < t_{\kappa}^r < \cdots$ .

In the following, we will show that  $t_{\kappa}^r \to \infty$  as  $\kappa \to \infty$  to exclude Zeno behavior. There are two possibilities for every actual impulsive instant. Firstly, if  $t_{\kappa}^r = t_{\kappa-1}^r + \Delta$ , one has

$$t_{\kappa}^{r} - t_{\kappa-1}^{r} = \Delta,$$

which naturally excludes the Zeno behavior.

Secondly, if  $t_{\kappa}^r = t_{\kappa}^{*r}$ , we construct an auxiliary function  $U^r(t) = \exp(t)\mathcal{E}V^r(t)$ ,  $t \in [t_{\kappa-1}^r, t_{\kappa}^r)$ . Calculate the upper-right Dini derivative of  $U^r(t)$ . In view of condition (8), it yields that

$$D^{+}U^{r}(t) = \exp(t) \mathcal{E}V^{r}(t) + \exp(t) \mathcal{E}\mathcal{L}V^{r}(t)$$
  
$$\leq (1 + \sigma_{1}) \exp(t) \mathcal{E}V^{r}(t) = (1 + \sigma_{1})U^{r}(t).$$
(9)

That is,  $t_{\kappa}^{r} = t_{\kappa}^{*r}$ , then it can be derived from (6) and (9) that

$$\exp(a_{\kappa}) \mathcal{E}V^{r} (t_{\kappa-1}^{r}) \leqslant \mathcal{E}V^{r} (t_{\kappa}^{r-}) = \mathcal{E}V^{r} (t_{\kappa}^{*r-})$$

$$\leqslant \exp((1+\sigma_{1})(t_{\kappa}^{r}-t_{\kappa-1}^{r})) \mathcal{E}V^{r} (t_{\kappa-1}^{r}). \tag{10}$$

From (10) we have that

$$t_{\kappa}^r - t_{\kappa-1}^r \geqslant \frac{a_{\kappa}}{1 + \sigma_1}.$$

Thus, the following inequality always holds:

$$t_{\kappa}^{r} - t_{\kappa-1}^{r} \geqslant \min \left\{ \frac{a_{\kappa}}{1 + \sigma_{1}}, \Delta \right\}.$$

Further, in view of  $\sum_{i=1}^{\kappa} a_i \to \infty$  as  $\kappa \to \infty$ , one can obtain

$$t_{\kappa}^{r} \geqslant \min \left\{ \sum_{i=1}^{\kappa} \frac{a_{i}}{1+\sigma_{1}}, \kappa \Delta \right\} + t_{0}^{r} \to \infty \quad \text{as } \kappa \to \infty.$$
 (11)

Thus, Zeno behavior of system (1) under event-triggered mechanism (5) is excluded. □

**Remark 8.** Zeno behavior occurs when an infinite number of operations take place within a finite time frame. The presence of Zeno behavior can lead to system instability. Therefore, it is important to demonstrate the absence of Zeno behavior for ensuring the effectiveness of the ETM before assessing system stability. The paper introduces Theorem 1, defining the ETM separately for nodes in each layer using Lyapunov function, and establishes conditions for system (1) to prevent Zeno behavior. Unlike the literature [20, 24, 25], the exclusion of Zeno behaviour in this paper is divided into two cases. The first is the case where there is no trigger event (6) within the predefined impulsive interval  $\Delta$ , whose a minimum positive lower bound is the predefined impulsive interval  $\Delta$ . The other case is the case where the trigger event (6) is triggered and a minimum positive lower bound is found to be  $a_{\kappa}/(1+\sigma_1)$ . The predefined impulsive interval  $\Delta$  in the control strategy ensures that the system is forced to be controlled, which has the advantage of reduced resource waste and faster convergence time.

**Theorem 2.** Based on Assumptions 1 and 2, networks (1) and (2) can reach intralayer synchronization under ETDIC (4) with (5) if there exist positive definite matrix  $Q \in \mathbb{R}^{n \times n}$ , positive diagonal matrix  $\Pi_1 \in \mathbb{R}^{n \times n}$ , and positive scalars d,  $\tau$ ,  $\tau_{\kappa}$   $\eta_1$ ,  $\Delta$ , and  $a_{\kappa}$  with  $a_{\kappa} \geqslant (1 + \sigma_1)\tau$  such that

$$I_N \otimes \left[ \left( -2C - \eta_1 I_n + B \Pi_1^{-1} B^{\mathrm{T}} + Q^{\mathrm{T}} \Pi_1 Q + \mu I_n \right) \right] - 2\alpha (L^r \otimes H) \leqslant 0, \tag{12}$$

$$\begin{bmatrix} -\exp(-d)I_n & K^{\mathrm{T}} \\ * & -I_n \end{bmatrix} \leqslant 0, \tag{13}$$

$$\Delta < \inf_{\kappa \in Z_+} \left\{ \tau_{\kappa} + \frac{d}{1 + \sigma_1} \right\},\tag{14}$$

where

$$\sigma_1 = \eta_1 + \beta \lambda_{\max}(\Gamma) M d^*, \quad d^* = \max_{1 \leqslant r, k \leqslant M} \{d_{rk}\}.$$

*Proof.* Consider the following Lyapunov function:

$$V(t) = e^{T}(t)e(t) = \sum_{r=1}^{M} V^{r}(t) = \sum_{r=1}^{M} \sum_{i=1}^{N} (e_{i}^{r}(t))^{T} e_{i}^{r}(t).$$

On the one hand, for all  $t \in [t_{\kappa}^r, t_{\kappa+1}^r)$  and for all  $\kappa \in Z^+$ , it always holds that

$$\mathcal{L}V^{r}(t) = 2\sum_{i=1}^{N} (e_{i}^{r}(t))^{T} \left[ -Ce_{i}^{r}(t) + Bf(e_{i}^{r}(t)) - \alpha \sum_{j=1}^{N} l_{ij}^{r} He_{j}^{r}(t) - \beta \sum_{k=1}^{M} d_{rk} \Gamma e_{i}^{k}(t) \right] + \sum_{i=1}^{N} \operatorname{trace}(g^{T}(t, e_{i}^{r}(t))g(t, e_{i}^{r}(t))).$$
(15)

Based on Assumption 1 and Lemma 1, one can obtain

$$2\sum_{i=1}^{N} (e_{i}^{r}(t))^{T} B f(e_{i}^{r}(t))$$

$$\leq \sum_{i=1}^{N} [(e_{i}^{r}(t))^{T} B \Pi_{1}^{-1} B^{T} e_{i}^{r}(t) + f^{T}(e_{i}^{r}(t)) \Pi_{1} f(e_{i}^{r}(t))]$$

$$\leq \sum_{i=1}^{N} (e_{i}^{r}(t))^{T} [B \Pi_{1}^{-1} B^{T} + Q^{T} \Pi_{1} Q] e_{i}^{r}(t)$$

$$= (e^{r}(t))^{T} [B \Pi_{1}^{-1} B^{T} + Q^{T} \Pi_{1} Q] e^{r}(t).$$
(16)

We can get the following equality about coupled term:

$$-2\alpha \sum_{i=1}^{N} \left( e_i^r(t) \right)^{\mathrm{T}} \sum_{i=1}^{N} l_{ij}^r H e_j^r(t) = -2\alpha \left( e^r(t) \right)^{\mathrm{T}} (L^r \otimes H) e^r(t)$$
 (17)

and

$$-2\beta \sum_{i=1}^{N} (e_{i}^{r}(t))^{T} \sum_{k=1}^{M} d_{rk} \Gamma e_{i}^{k}(t)$$

$$\leq \beta \lambda_{\max}(\Gamma) \sum_{i=1}^{N} \sum_{k=1}^{M} d_{rk} (\|e_{i}^{r}(t)\|^{2} + \|e_{i}^{k}(t)\|^{2})$$

$$\leq \beta \lambda_{\max}(\Gamma) M d^{*} \|e^{r}(t)\|^{2}. \tag{18}$$

Based on Assumption 2, one has

$$\sum_{i=1}^{N} \operatorname{trace}\left(g^{\mathrm{T}}\left(t, e_{i}^{r}(t)\right)g\left(t, e_{i}^{r}(t)\right)\right)$$

$$\leq \mu \sum_{i=1}^{N} \left(e_{i}^{r}(t)\right)^{\mathrm{T}} e_{i}^{r}(t) = \mu \left(e^{r}(t)\right)^{\mathrm{T}} e^{r}(t). \tag{19}$$

From (16)–(18) we have

$$\mathcal{L}V^{r}(t) = \left(e^{r}(t)\right)^{T} \left[I_{N} \otimes \left(-2C + B\Pi_{1}^{-1}B^{T} + Q^{T}\Pi_{1}Q + \mu I_{n}\right) - 2\alpha(L^{r} \otimes H)\right]e^{r}(t) + \beta\lambda_{\max}(\Gamma)Md^{*}\left\|e^{r}(t)\right\|^{2}$$

$$\leq \eta_{1}\left\|e^{r}(t)\right\|^{2} + \beta\lambda_{\max}(\Gamma)Md^{*}\left\|e^{r}(t)\right\|^{2} = \sigma_{1}V^{r}(t).$$
(20)

According to (19), it yields

$$\mathcal{E}\mathcal{L}V(t) = \mathcal{E}\sum_{r=1}^{M} \mathcal{L}V^{r}(t) \leqslant \sigma_{1}\mathcal{E}\sum_{r=1}^{M} V^{r}(t) = \sigma_{1}\mathcal{E}V(t). \tag{21}$$

On the other hand, for  $t = t_{\kappa}^{r}$ , it follows from (13) that

$$\mathcal{E}V(t_{\kappa}^{r}) = \mathcal{E}\sum_{r=1}^{M} \sum_{i=1}^{N} \left(e_{i}^{r}(t_{\kappa}^{r})\right)^{\mathrm{T}} e_{i}^{r}(t_{\kappa}^{r})$$

$$= \mathcal{E}\sum_{r=1}^{M} \sum_{i=1}^{N} \left(e_{i}^{r}(t_{\kappa}^{r} - \tau_{\kappa})\right)^{\mathrm{T}} K^{\mathrm{T}} K e_{i}^{r}(t_{\kappa}^{r} - \tau_{\kappa})$$

$$\leq \exp(-d)\mathcal{E}\sum_{r=1}^{M} \sum_{i=1}^{N} \left(e_{i}^{r}(t_{\kappa}^{r} - \tau_{\kappa})\right)^{\mathrm{T}} e_{i}^{r}(t_{\kappa}^{r} - \tau_{\kappa})$$

$$= \exp(-d)\mathcal{E}V(t_{\kappa}^{r} - \tau_{\kappa}). \tag{22}$$

Based on Theorem 1, note that  $\Delta \geqslant \tau$ ,  $a_{\kappa} \geqslant (1+\sigma_1)\tau$  for all  $\kappa \in Z^+$ . Then one can obtain  $t_{\kappa}^r - t_{\kappa-1}^r \geqslant \min\left\{\tau_{\kappa}, \tau\right\} = \tau_{\kappa}$ , which implies that

$$t_{\kappa}^r - \tau_{\kappa} \geqslant t_{\kappa-1}^r \quad \forall \kappa \in Z^+.$$
 (23)

From (14) there exists a sufficiently small constant  $\varepsilon > 0$  such that

$$\Delta \leqslant \inf_{\kappa \in Z_+} \left\{ \frac{(1+\sigma_1)\tau_{\kappa} + d}{(1+\varepsilon)(1+\sigma_1)} \right\} < \inf_{\kappa \in Z_+} \left\{ \tau_{\kappa} + \frac{d}{1+\sigma_1} \right\},$$

by which we have

$$\Delta \leqslant \frac{(1+\sigma_1)\tau_{\kappa}+d}{(1+\varepsilon)(1+\sigma_1)} \quad \forall \kappa \in Z^+.$$

Then from the definition of event-triggered mechanism (5) we know whether the impulsive instant  $t_{\kappa}^{r}=t_{\kappa}^{*r}$  or  $t_{\kappa}^{r}=t_{\kappa-1}^{r}+\Delta$ . The following inequality always holds:

$$t_{\kappa}^{r} - t_{0}^{r} \leqslant \kappa \Delta \leqslant \frac{(1 + \sigma_{1}) \sum_{i=1}^{\kappa} \tau_{i} + \kappa d}{(1 + \sigma_{1})(1 + \varepsilon)} \quad \forall \kappa \in Z^{+}.$$
 (24)

Thus, at the first impulsive instant  $t_1^r$ , one has

$$t_1^r - t_0^r \leqslant \Delta \leqslant \frac{(1+\sigma_1)\tau_1 + d}{(1+\sigma_1)(1+\varepsilon)}.$$
 (25)

Further, it yields from (20)–(23) that

$$\mathcal{E}V(t_1^r) \leqslant \exp(-d)\mathcal{E}V(t_1^r - \tau_1)$$

$$\leqslant \exp(-d + (1 + \sigma_1)(t_1^r - \tau_1 - t_0^r))\mathcal{E}V(t_0^r), \tag{26}$$

which, together with (25), leads to

$$\mathcal{E}V(t_1^r) \leqslant \exp(-\varepsilon(1+\sigma_1)(t_1^r-t_0^r))\mathcal{E}V(t_0^r).$$

Similarly, at the second impulsive instant  $t_2^r$ , by (24), one has

$$t_2^r - t_0^r \leqslant 2\Delta \leqslant \frac{(1+\sigma_1)(\tau_1 + \tau_2) + 2d}{(1+\sigma_1)(1+\varepsilon)}.$$

Combining with (26), one has

$$\begin{split} \mathcal{E}V\left(t_{2}^{r}\right) &\leqslant \exp(-d)\mathcal{E}V\left(t_{2}^{r} - \tau_{2}\right) \\ &\leqslant \exp\left(-d + (1 + \sigma_{1})\left(t_{2}^{r} - \tau_{2} - t_{1}^{r}\right)\right)\mathcal{E}V\left(t_{1}^{r}\right) \\ &\leqslant \exp\left(-2d + (1 + \sigma_{1})\left(t_{2}^{r} - \tau_{1} - \tau_{2} - t_{0}^{r}\right)\right)\mathcal{E}V\left(t_{0}^{r}\right) \\ &\leqslant \exp\left(-\varepsilon(1 + \sigma_{1})\left(t_{2}^{r} - t_{0}^{r}\right)\right)\mathcal{E}V\left(t_{0}^{r}\right). \end{split}$$

By mathematical introduction, for any impulsive instant  $t_{\kappa}^{r}$ , it can be finally deduced from (24) that

$$\mathcal{E}V\left(t_{\kappa}^{r}\right) \leqslant \exp(-d)\mathcal{E}V\left(t_{\kappa}^{r} - \tau_{\kappa}\right)$$

$$\leqslant \exp\left(-d + (1 + \sigma_{1})\left(t_{\kappa}^{r} - \tau_{\kappa} - t_{\kappa-1}^{r}\right)\right)\mathcal{E}V\left(t_{\kappa-1}^{r}\right)$$

$$\leqslant \cdots \leqslant \exp\left(-\kappa d + (1 + \sigma_{1})\left(t_{\kappa}^{r} - \sum_{i=1}^{\kappa} \tau_{i} - t_{0}^{r}\right)\right)\mathcal{E}V\left(t_{0}^{r}\right)$$

$$\leqslant \exp\left(-\varepsilon(1 + \sigma_{1})\left(t_{\kappa}^{r} - t_{0}^{r}\right)\right)\mathcal{E}V\left(t_{0}^{r}\right) \quad \forall \kappa \in \mathbb{Z}^{+}.$$
(27)

In view of (11), when  $\kappa \to \infty$ , one has

$$t_{\kappa}^{r} - t_{0}^{r} \geqslant \min \left\{ \sum_{i=1}^{\kappa} \frac{a_{i}}{(1+\sigma_{1})}, \, \kappa \Delta \right\} \to \infty.$$
 (28)

From (11) and (27), for any  $t \in [t_{\kappa-1}^r, t_{\kappa}^r]$ ,

$$\begin{split} \mathcal{E}V(t) &\leqslant \exp\left((1+\sigma_1)\left(t-t_{\kappa-1}^r\right)\right) \mathcal{E}V\left(t_{\kappa-1}^r\right) \\ &\leqslant \exp\left(\Delta(1+\sigma_1)-\varepsilon(1+\sigma_1)\left(t_{\kappa-1}^r-t_0^r\right)\right) \mathcal{E}V\left(t_0^r\right) \\ &\leqslant \exp\left(\Delta(1+\sigma_1)-\varepsilon(1+\sigma_1)\min\left\{\sum_{i=1}^{\kappa-1}\frac{a_i}{(1+\sigma_1)},\,(\kappa-1)\Delta\right\}\right) \mathcal{E}V\left(t_0^r\right). \end{split}$$

It can be derived from (28) that  $\mathcal{E}V(t) \to 0$  as  $\kappa \to \infty$ , which implies that networks (1) and (2) realize the intra-layer synchronization under proposed ETDIC (4) with (5).

**Remark 9.** In contrast to prior works [5, 25], our article introduces a stochastic perturbation term and applies Itô's formula to the Lyapunov function, which lacks normal differentiation. We address Zeno behavior by introducing an auxiliary function, inspired by [32], effectively resolving issues arising from the perturbation term. This method ensures consistent positive lower bounds for inter-event times, leading to the following conclusions.

When the triggering parameter  $a_{\kappa}$  does not vary with the impulsive instants, i.e.,  $a_{\kappa}=a$ , Theorem 1 can degenerate into the following corollary.

**Corollary 1.** Based on Assumptions 1 and 2, networks (1) and (2) can reach intra-layer synchronization under ETDIC (4) with (5), while avoiding the Zeno phenomenon, if there exist positive definite matrix  $Q \in \mathbb{R}^{n \times n}$ , positive diagonal matrix  $\Pi_1 \in \mathbb{R}^{n \times n}$ , and positive scalars d,  $\tau$ ,  $\tau_{\kappa}$ ,  $\eta_1$ ,  $\Delta$ , and a with  $a \geqslant (1 + \sigma_1)\tau$  such that

$$I_N \otimes \left[ \left( -2C - \eta_1 I_n + B \Pi_1^{-1} B^{\mathrm{T}} + Q^{\mathrm{T}} \Pi_1 Q + \mu I_n \right) \right] - 2\alpha \left( L^r \otimes H \right) \leqslant 0,$$

$$\begin{bmatrix} -\exp\left( -d \right) I_n & K^{\mathrm{T}} \\ * & -I_n \end{bmatrix} \leqslant 0, \qquad \Delta < \inf_{\kappa \in Z_+} \left\{ \tau_\kappa + \frac{d}{1+\sigma_1} \right\},$$

where

$$\sigma_1 = \eta_1 + \beta \lambda_{\max}(\Gamma) M d^*, \qquad d^* = \max_{1 \leqslant r, k \leqslant M} \{d_{rk}\}.$$

Moreover, the impulse time sequence  $\{t_{\kappa}^r\}$  satisfies

$$t_{\kappa}^r - t_{\kappa-1}^r \geqslant \min\left\{\frac{a}{1+\sigma_1}, \Delta\right\} \quad \forall \kappa \in \mathbb{Z}^+.$$

**Remark 10.** Note that for the conditions  $t_{\kappa}^r - t_{\kappa-1}^r \geqslant \min\{a_{\kappa}/(1+\sigma_1), \Delta\}$  in Theorem 1 and  $\Delta < \inf_{\kappa \in Z_+} \{\tau_{\kappa} + d/(1+\sigma_1)\}$  in Theorem 2, if the trigger condition (6) is triggered, a relationship between the trigger parameter, impulsive interval, impulsive parameter, and time delay can be deduced:  $a_{\kappa} \leqslant (1+\sigma_1)\Delta \leqslant (1+\sigma_1)\tau_{\kappa} + d$ . The results demonstrate that the time delay impacts not only the intra-layer synchronization of the system but also the gain of the impulse in the controller (4).

#### 3.2 Inter-layer synchronization

In this section, inter-layer synchronization is considered. The tracking target  $s_i$  of the *i*th node in each layer of system (1) is designed as follows:

$$ds_i(t) = \left[ -Cs_i(t) + Bf(s_i(t)) - \alpha \sum_{i=1}^{N} l_{ij}^r Hs_j(t) \right] dt + g(t, s_i(t)) dw(t).$$
 (29)

Define synchronization error  $e_i^r(t) = x_i^r(t) - s_i(t)$ . For achieving inter-layer synchronization of networks (1), the ETDIC scheme is characterized as

$$u_i^r(t) = \sum_{\kappa=1}^{\infty} \left( K e_i^r(t - \tau_\kappa) - e_i^r(t) \right) \delta(t - t_\kappa^i), \quad \kappa \in \mathbb{Z}^+.$$
 (30)

According to networks (1) and (29), the error system is

$$de_{i}^{r}(t) = \left[ -Ce_{i}^{r}(t) + Bf(e_{i}^{r}(t)) - \alpha \sum_{j=1}^{N} l_{ij}^{r} He_{j}^{r}(t) - \beta \sum_{j=1}^{N} l_{ij}^{r} He_{i}^{r}(t) \right] dt + g(t, e_{i}^{r}(t)) dw(t), \quad t \neq t_{\kappa}^{i},$$

$$e_{i}^{r}(t) = Ke_{i}^{r}(t^{-} - \tau_{\kappa}), \quad t = t_{\kappa}^{i},$$
(31)

where  $t_{\kappa}^{i}$  is the impulsive instant at the ith node of each layer, which is determined by

$$t_{\kappa}^{i} = \min\{\widetilde{t}_{\kappa}^{i}, t_{\kappa-1}^{i} + \Delta\},$$

$$\widetilde{t}_{\kappa}^{i} = \inf\{t \geqslant t_{\kappa-1}^{i} \colon \mathcal{E}V_{i}(t) \geqslant \exp(a_{\kappa})\mathcal{E}V_{i}(t_{\kappa-1}^{i})\}.$$
(32)

Here  $\mathcal{E}V_i(t) = \mathcal{E}\sum_{r=1}^M (e_i^r(t))^{\mathrm{T}} e_i^r(t) = \mathcal{E}(e_i(t))^{\mathrm{T}} e_i(t)$ , and  $\widetilde{t}_{\kappa}^i$  is the event-triggered impulsive instant at the ith node of each layer.

**Definition 2.** Networks (1) and (29) are said to achieve inter-layer synchronization under ETDIC (30) with (32) if  $\lim_{t\to\infty} \|x_i^r(t) - s_i(t)\| = 0$ , i = 1, 2, ..., N, r = 1, 2, ..., M.

**Theorem 3.** Based on Assumptions 1 and 2, networks (1) and (29) can reach inter-layer synchronization under ETDIC (30) with (32), while avoiding the Zeno phenomenon, if there exist positive definite matrix  $Q \in \mathbb{R}^{n \times n}$ , positive diagonal matrix  $\Pi_1 \in \mathbb{R}^{n \times n}$ , and positive scalars d,  $\tau$ ,  $\tau_{\kappa}$ ,  $\eta_2$ ,  $\Delta$ , and  $a_{\kappa}$  with  $a_{\kappa} \geqslant (1 + \sigma_2)\tau$  such that

$$I_{M} \otimes \left[ \left( -2C - \eta_{2}I_{n} + B\Pi_{1}^{-1}B^{T} + Q^{T}\Pi_{1}Q + \mu I_{n} \right) \right] - 2\beta(D \otimes \Gamma) \leqslant 0,$$

$$\begin{bmatrix} -\exp\left(-d\right)I_{n} & K^{T} \\ * & -I_{n} \end{bmatrix} \leqslant 0, \qquad \Delta < \inf_{\kappa \in Z_{+}} \left\{ \tau_{\kappa} + \frac{d}{1 + \sigma_{2}} \right\},$$

where

$$\sigma_2 = \eta_2 + \alpha \lambda_{\max}(H)Nl^*, \quad l^* = \max_{i,j,r} \{l_{ij}^r\}.$$

Moreover, the impulse time sequence  $\{t_{\kappa}^i\}$  satisfies

$$t_{\kappa}^{i} - t_{\kappa-1}^{i} \geqslant \min \left\{ \frac{a_{\kappa}}{1 + \sigma_{2}}, \Delta \right\} \quad \forall \kappa \in \mathbb{Z}^{+}.$$

*Proof.* Consider the following Lyapunov function:

$$V(t) = e^{T}(t)e(t) = \sum_{i=1}^{N} V_i(t) = \sum_{r=1}^{M} \sum_{i=1}^{N} \left(e_i^r(t)\right)^{T} e_i^r(t).$$

On the one hand, for all  $t\in [t^i_\kappa, t^i_{\kappa+1})$  and all  $\kappa\in Z^+$ , it always holds that

$$\mathcal{L}V_{i}(t) = 2\sum_{r=1}^{M} (e_{i}^{r}(t))^{T} \left[ -Ce_{i}^{r}(t) + Bf(e_{i}^{r}(t)) - \alpha \sum_{j=1}^{N} l_{ij}^{r} He_{j}^{r}(t) - \beta \sum_{k=1}^{M} d_{rk} \Gamma e_{i}^{k}(t) \right] + \sum_{r=1}^{M} \operatorname{trace}(g^{T}(t, e_{i}^{r}(t))g(t, e_{i}^{r}(t))).$$
(33)

Based on Assumption 1 and Lemma 1, one can obtain

$$2\sum_{r=1}^{M} (e_{i}^{r}(t))^{T} B f(e_{i}^{r}(t))$$

$$\leq \sum_{r=1}^{M} [(e_{i}^{r}(t))^{T} B \Pi_{1}^{-1} B^{T} e_{i}^{r}(t) + f^{T}(e_{i}^{r}(t)) \Pi_{1} f(e_{i}^{r}(t))]$$

$$\leq \sum_{r=1}^{M} (e_{i}^{r}(t))^{T} [B \Pi_{1}^{-1} B^{T} + Q^{T} \Pi_{1} Q] e_{i}^{r}(t)$$

$$= (e_{i}(t))^{T} [I_{M} \otimes (B \Pi_{1}^{-1} B^{T} + Q^{T} \Pi_{1} Q)] e_{i}(t)$$
(34)

and

$$-2\alpha \sum_{r=1}^{M} (e_{i}^{r}(t))^{T} \sum_{j=1}^{N} l_{ij}^{r} H e_{j}^{r}(t)$$

$$\leq \alpha \lambda_{\max}(H) \sum_{r=1}^{M} \sum_{j=1}^{N} l_{ij}^{r} (\|e_{i}^{r}(t)\|^{2} + \|e_{j}^{r}(t)\|^{2})$$

$$\leq \alpha \lambda_{\max}(H) N l^{*} \|e_{i}(t)\|^{2}. \tag{35}$$

Moreover,

$$-2\beta \sum_{r=1}^{M} \left(e_i^r(t)\right)^{\mathrm{T}} \sum_{k=1}^{M} d_{rk} \Gamma e_i^k(t) = -2\beta \left(e_i(t)\right)^{\mathrm{T}} (D \otimes \Gamma) e_i(t). \tag{36}$$

Based on Assumption 2, one has

$$\sum_{r=1}^{M} \operatorname{trace} \left( g^{\mathrm{T}}(t, e_i^r(t)) g(t, e_i^r(t)) \right)$$

$$\leq \mu \sum_{r=1}^{M} (e_i^r(t))^{\mathrm{T}} e_i^r(t) = \mu(e_i(t))^{\mathrm{T}} e_i(t). \tag{37}$$

From (33)–(36) we have

$$\mathcal{L}V_{i}(t) = \left(e_{i}(t)\right)^{\mathrm{T}} \left[I_{M} \otimes \left(-2C + B\Pi_{1}^{-1}B^{\mathrm{T}} + Q^{\mathrm{T}}\Pi_{1}Q + \mu I_{n}\right) - 2\beta(D \otimes \Gamma)\right] e_{i}(t) + \alpha \lambda_{\max}(H)Nl^{*} \left\|e_{i}^{k}(t)\right\|^{2}$$

$$\leq \eta_{2} \left\|e_{i}(t)\right\|^{2} + \alpha \lambda_{\max}(H)Nl^{*} \left\|e_{i}(t)\right\|^{2}$$

$$= \sigma_{2}V_{i}(t). \tag{38}$$

It follows from (37) that

$$\mathcal{EL}V(t) = \mathcal{E}\sum_{i=1}^{N} \mathcal{L}V_i(t) \leqslant \sigma_2 \mathcal{E}\sum_{i=1}^{N} V_i(t) = \sigma_2 \mathcal{E}V(t).$$

The rest of the proof is similar to that of Theorem 2, then networks (1) and (29) can reach inter-layer synchronization under ETDIC (30) with (32). We can see that (37) satisfies condition (8) of Theorem 1. Moreover, when the condition  $a_{\kappa} \geq (1 + \sigma_2)\tau$  is met, the error system (31) can avoid Zeno behavior. So, the impulse time sequence  $\{t_{\kappa}^i\}$  satisfies  $t_{\kappa}^i - t_{\kappa-1}^i \geq \min\{a_{\kappa}/(1 + \sigma_2), \Delta\}$  for all  $\kappa \in Z^+$ .

**Corollary 2.** Based on Assumptions 1 and 2, networks (1) and (29) can reach inter-layer synchronization under ETDIC (30) with (32), while avoiding the Zeno phenomenon, if there exist positive definite matrix  $Q \in \mathbb{R}^{n \times n}$ , positive diagonal matrix  $\Pi_1 \in \mathbb{R}^{n \times n}$ , and positive scalars d,  $\tau$ ,  $\tau_\kappa$ ,  $\eta_2$ ,  $\Delta$  and a with  $a \ge (1 + \sigma_2)\tau$  such that

$$I_{M} \otimes \left[ \left( -2C - \eta_{2}I_{n} + B\Pi_{1}^{-1}B^{\mathrm{T}} + Q^{\mathrm{T}}\Pi_{1}Q + \mu I_{n} \right) \right] - 2\beta(D \otimes \Gamma) \leqslant 0,$$

$$\begin{bmatrix} -\exp\left(-d\right)I_{n} & K^{\mathrm{T}} \\ * & -I_{n} \end{bmatrix} \leqslant 0, \qquad \Delta < \inf_{\kappa \in Z_{+}} \left\{ \tau_{\kappa} + \frac{d}{1 + \sigma_{2}} \right\},$$

where

$$\sigma_2 = \eta_2 + \alpha \lambda_{\max}(H)Nl^*, \qquad l^* = \max_{i,j,r} \{l_{ij}^r\}.$$

Moreover, the impulse time sequence  $\{t_{\kappa}^i\}$  satisfies

$$t_{\kappa}^{i} - t_{\kappa-1}^{i} \geqslant \min \left\{ \frac{a_{\kappa}}{1 + \sigma_{2}}, \Delta \right\} \quad \forall \kappa \in \mathbb{Z}^{+}.$$

**Remark 11.** In this paper, matrices H and  $\Gamma$  are assumed to be symmetric. However, if the constructed Lyapunov function does not consider localization, matrices H and  $\Gamma$  can be arbitrary square matrices.

**Remark 12.** The study of inter-layer synchronization considers the relationship between the states of the layers and does not consider the states within the layers. Unlike intralayer synchronization, we construct Lyapunov function that relates the states between corresponding nodes in each layer. Corollary 2 is a special case of Theorem 3.

**Remark 13.** This study addresses key challenges including the limited predictability of ETDIC, the neglect of time delays in traditional impulsive control, and the conservative synchronization criteria for stochastic multi-layer networks through a hybrid triggering mechanism, decoupled multi-layer coupling modeling, and innovative theoretical tools. The proposed control strategy and synchronization conditions remain fully applicable when the multi-layer network degenerates to a single-layer structure. Moreover, the control mechanism innovation (predefined impulse intervals) effectively resolves the Zeno problem in ETDIC for single-layer systems.

**Remark 14.** Multi-layer network modelling is the core framework for solving collaboration bottlenecks in modern systems engineering, while intra/inter-layer synchronization control is the theoretical cornerstone for ensuring its robust operation. Compatibility of ETDIC strategies in multi-layer and single-layer scenarios provides a smooth path for technology migration.

## 4 Numerical simulations

#### 4.1 Example about ETIC-PII

Consider the SMLNs depicted by

$$dx_{i}^{r}(t) = \left[ -Cx_{i}^{r}(t) + Bf(x_{i}^{r}(t)) - \alpha \sum_{j=1}^{6} l_{ij}^{r} Hx_{j}^{r}(t) - \beta \sum_{k=1}^{3} d_{rk} \Gamma x_{i}^{k}(t) + u_{i}^{r}(t) \right] dt + g(t, x_{i}^{r}(t)) dw(t),$$
(39)

where  $x_i^r(t) = (x_{i1}^r(t), x_{i2}^r(t), x_{i3}^r(t))^{\mathrm{T}}$ ,  $C = \mathrm{diag}(3,3,3)$ ,  $\alpha = 0.02$ ,  $\beta = 0.9$ ,  $f(x_i^r) = (\mathrm{tanh}(x_{i1}^r), \mathrm{tanh}(x_{i2}^r), \mathrm{tanh}(x_{i3}^r))^{\mathrm{T}}$ ,  $i = 1, 2, \ldots, 6$ , r = 1, 2, 3,

$$B = \begin{bmatrix} 1.31 & -0.46 & -1.24 \\ -1.26 & 0.46 & -1.06 \\ -0.43 & 0.54 & 1.06 \end{bmatrix},$$

$$H = \begin{bmatrix} 1 & 2 & -1 \\ 2 & 0 & 0 \\ -1 & 0 & 3 \end{bmatrix}, \qquad \Gamma = \begin{bmatrix} 0 & -1 & -2 \\ -1 & 1 & 0 \\ -2 & 0 & 1 \end{bmatrix}.$$

The topology of network (39) is shown in Fig. 2. Meanwhile, the corresponding Laplacian matrices  $L^1$ ,  $L^2$ , and  $L^3$  of each layer representing the intra-layer topology are given as

$$L^{1} = \begin{bmatrix} 3 & -1 & -1 & 0 & -1 & 0 \\ -1 & 4 & -1 & -1 & -1 & 0 \\ -1 & -1 & 4 & 0 & -1 & -1 \\ 0 & -1 & 0 & 2 & 0 & -1 \\ -1 & -1 & -1 & 0 & 3 & 0 \\ 0 & 0 & -1 & -1 & 0 & 2 \end{bmatrix}, \qquad L^{2} = \begin{bmatrix} 2 & -1 & 0 & 0 & -1 & 0 \\ -1 & 1 & 0 & 0 & 0 & 0 \\ 0 & 0 & 3 & -1 & -1 & -1 \\ 0 & 0 & -1 & 1 & 0 & 0 \\ -1 & 0 & -1 & 0 & 3 & -1 \\ 0 & 0 & -1 & 0 & -1 & 2 \end{bmatrix},$$

and

$$L^{3} = \begin{bmatrix} 1 & 0 & 0 & 0 & 0 & -1 \\ 0 & 2 & 0 & -1 & 0 & -1 \\ 0 & 0 & 2 & -1 & -1 & 0 \\ 0 & -1 & -1 & 3 & 0 & -1 \\ 0 & 0 & -1 & 0 & 2 & -1 \\ -1 & -1 & 0 & -1 & -1 & 4 \end{bmatrix}.$$

The matrix D representing the inter-layer topology is described as

$$D = \begin{bmatrix} 1 & -1 & 0 \\ -1 & 2 & -1 \\ 0 & -1 & 1 \end{bmatrix}.$$

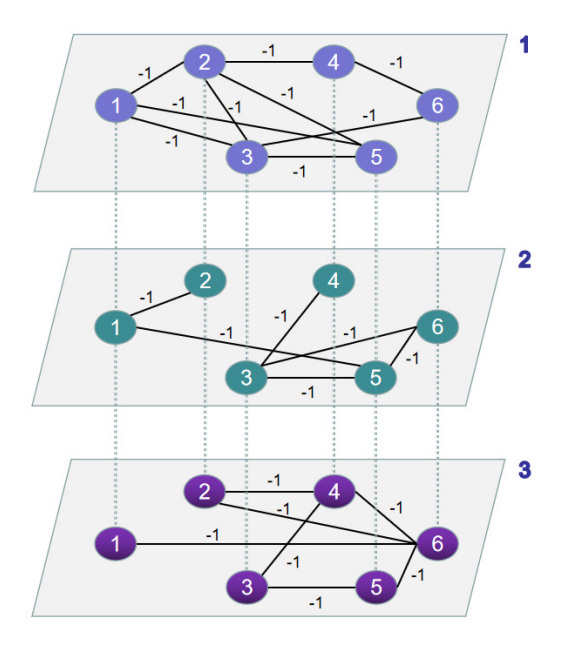


Figure 2. Topology structure of system (39) with 6 nodes and 3 layers.

Moreover, we select the noise intensity function  $g(t, e_i^r(t)) = 0.04e_i^r(t)$  and  $\mu = 0.08$ , then Assumption 2 holds.

## 4.1.1 Intra-layer synchronization

The intra-layer synchronization target  $s^r(t)$  depicted by

$$ds^{r}(t) = \left[ -Cs^{r}(t) + Bf(s^{r}(t)) - \beta \sum_{k=1}^{3} d_{rk} \Gamma s^{k}(t) \right] dt + g(t, s^{r}(t)) dw(t).$$
 (40)

The initial data of the synchronization state of target node in rth layer is set as  $s^1(t) = s^2(t) = s^3(t) = (-0.2, -0.5, 0.8)$ . When there is no control input, it can be observed from Fig. 3(a) that the intra-layer synchronization between network (38) and the target system (39) cannot be achieved.

Now, to realize the intra-layer synchronization of system (39) and target system (40) under ETDIC (4) with (5), we choose triggering parameter a=0.06, impulsive interval  $\Delta=0.3$ , and time delay in impulses  $\tau_{\kappa}=0.05$ . Then impulse gain matrix  $K=0.6I_3$ .

Figure 3(b)) illustrates the progression of intra-layer synchronization error controlled by ETDIC (4) following event (5)–(6). Figure 4(a) displays the triggered instants when events occur at each layer using the event-triggered mechanism (6). Moreover, Fig. 4(b) shows the impulsive instants in each layer under ETDIC (4), where the symbol  $\otimes$  denotes event-triggered impulsive moment, while the symbol  $\circ$  represents forced impulsive

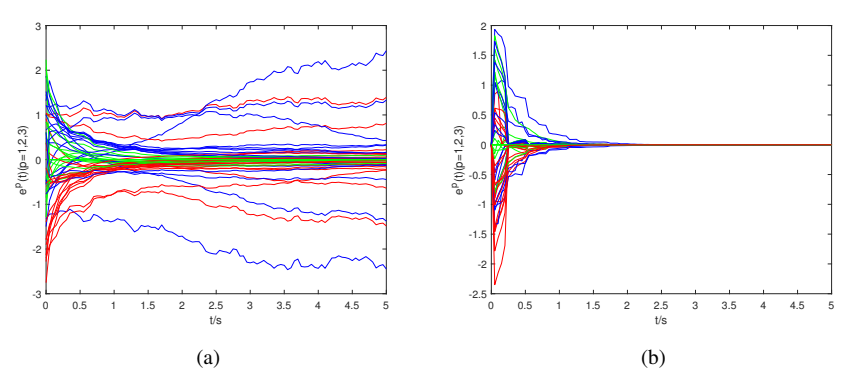


Figure 3. Time evolutions of intra-layer synchronization error  $e^p(t)$ , p=1,2,3: (a) without control; (b) with control (4).

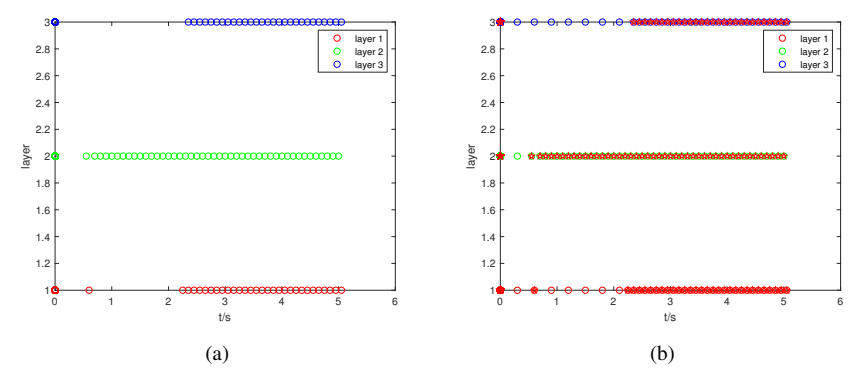


Figure 4. (a) Event-triggered instants for each layer; (b) impulsive instants for each layer.

instant. Figures 3–4 illustrate the effectiveness of the control strategy (4) and the event-triggered impulsive mechanism (5)–(6) proposed in this paper.

As depicted in Fig. 4(b), the first layer contains 6 forced impulsive moments. In the second layer, there is 1 forced impulsive moment. The third layer comprises 7 moments that do not meet the trigger condition (6) and are thus controlled by impulsive actions.

The following provides a detailed algorithm for the theorem to better understand the contents of the article.

#### **Algorithm 1.** The algorithm steps for Theorem 2.

**Step 1:** Initialize system parameters  $B, C, H, \Gamma, \alpha, \beta$ . Based on Assumptions 1 and 2, choose appropriate  $q, \mu$ .

**Step 2:** Use LMI toolbox in MATLAB and conditions (12) to solve feasible  $\Pi_1$ ,  $\eta_1$ ,  $\sigma_1$ .

**Step 3:** Provide control gain K to find the impulsive parameter d that satisfies condition (13).

**Step 4:** After determine time delay  $\tau_{\kappa}$ , provide impulsive interval  $\Delta$ , then verify condition (14).

**Step 5:** According to Remark 4, the value of the trigger parameter  $a_{\kappa}$  can be obtained.

**Step 6**: By judging the event-triggered mechanism (5), the intra-layer error  $e^p$  is made to reach a synchronized state.

#### 4.1.2 Inter-layer synchronization

The inter-layer synchronization target  $s_i(t)$  depicted by

$$ds_i(t) = \left[ -Cs_i(t) + Bf(s_i(t)) - \alpha \sum_{j=1}^6 l_{ij}^r Hs_j(t) \right] dt + g(t, s_i(t)) dw(t).$$
 (41)

The initial data of the synchronization state of ith node in each layer is set as  $s_i(t) = (-0.2, -0.5, 0.8)$ ,  $i = 1, 2, \dots, 6$ . In the absence of any control input, as depicted in Fig. 5(a), it is evident that the inter-layer synchronization between network (38) and the target system (40) cannot be attained.

To achieve intra-layer synchronization between system (39) and target system (41) using ETDIC (30) with (32), the following parameters are selected:  $a_1=a_6=0.02$ ,  $a_2=a_4=0.006$ ,  $a_3=a_5=0.06$ , and impulsive interval  $\Delta=0.3$ . Consequently, it is deduced that the impulse gain matrix  $K=0.6I_3$ .

Figures 5–6 depict the outcomes of the simulations. Specifically, in Fig. 5(b)), the time evolution of the inter-layer synchronization error controlled by ETDIC (30) following

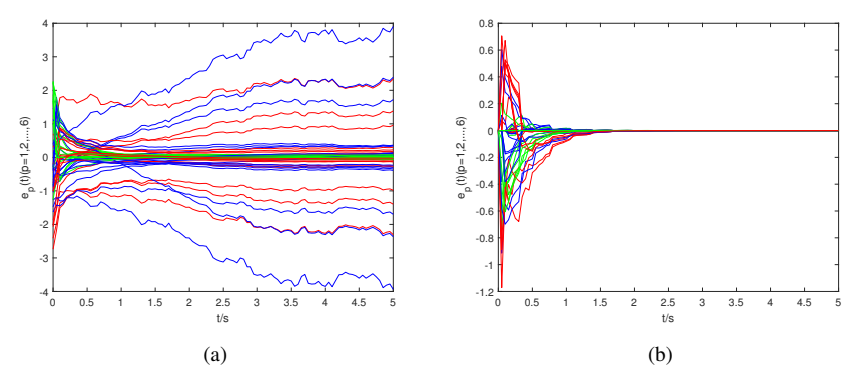


Figure 5. Time evolutions of inter-layer synchronization error  $e_p(t)$ , p = 1, 2, ..., 6: (a) without control; (b) with control (30).

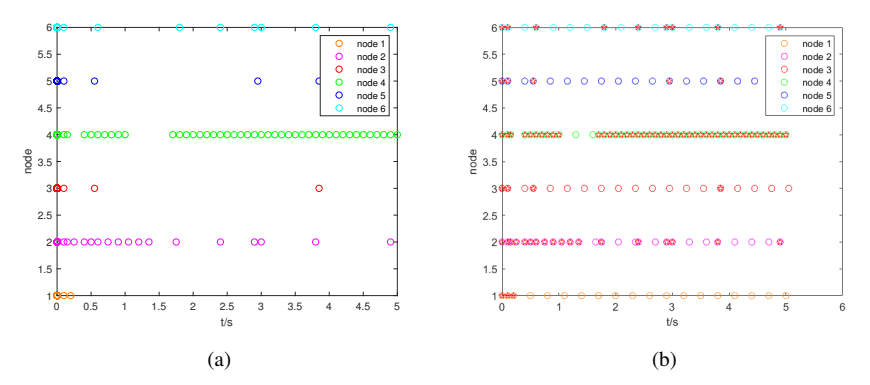


Figure 6. (a) Event-triggered instants; (b) impulsive instants.

event (32) is illustrated. Figure 6(a) displays the triggered instants of the ith node ( $i=1,2,\ldots,6$ ) in each layer. Additionally, Fig. 6(b) shows the impulsive instants of the ith node ( $i=1,2,\ldots,6$ ) in each layer under ETDIC (30), where the symbol 3 denotes event-triggered impulsive moment, while the symbol 3 represents forced impulsive instant.

In Figs. 4(a) and 6(a), the event-triggered instants are generated solely by triggering events. In contrast, the pulse instants in (b) correspond respectively to times generated by triggering events and predetermined time instants triggered to occur when no event happens within the predefined interval.

## 4.2 Example of a comparison between ETIC-PII and ETIC

Assuming that the other parameters of the network remain unchanged, consider the ETIC-PII and the existing event-triggered time-lag pulse control methods. For a better comparison, we will use the same nodes as in Section 4.1. In intra-layer synchronisation, two triggering mechanisms are considered, ETIC-PII (4) with (5) and ETDIC (4) with (6); while in inter-layer synchronisation, the event triggering mechanisms considered are similar to those of intra-layer synchronisation.

From Figs. 7(a) and 7(b) it can be found that the error intra-layer synchronisation under ETIC-PII (4) with (5) does not fluctuate further after it tends to 0. On the contrary, after the error intra-layer synchronisation under ETDIC (4) with (6) tends to 0, the event does not reach the triggering condition, and the error disperses, which suggests that the control effect of ETIC-PII (4) with (5) is stronger.

Figures 8(a) and 8(b) reveal that ETDIC-PII (4) with (30) exhibits fewer event-triggered instants per layer than ETDIC (4) with (31). This indicates that ETDIC (4) with (31) operates with higher control intensity, triggering events at elevated frequencies that incur significant resource consumption.

From Figs. 9(a) and 9(b) it can be found that the inter-layer synchronisation of errors under ETIC-PII (4) and (30) does not continue to fluctuate after converging to 0. On

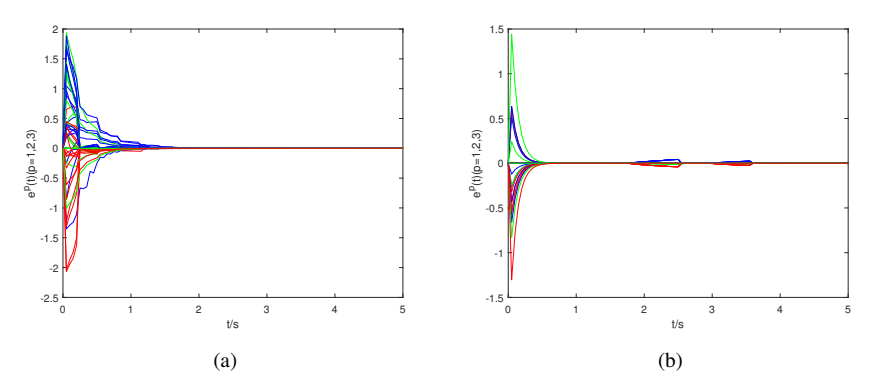


**Figure 7.** Time evolutions of intra-layer synchronization error  $e^p(t)$ , p=1,2,3: (a) ETIC-PII (4) with (5); (b) ETDIC (4) with (6).

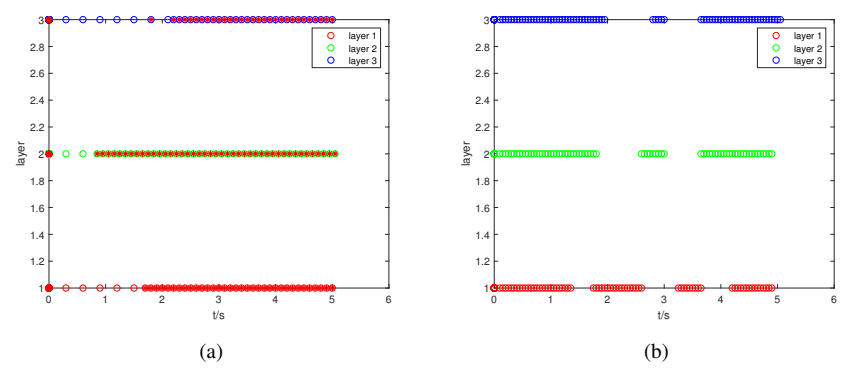
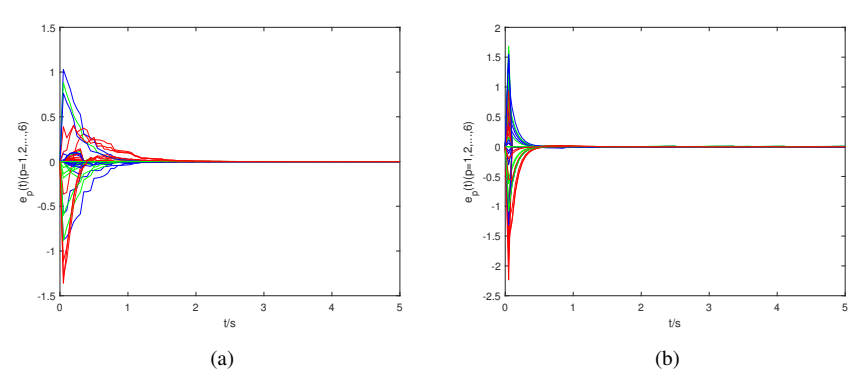


Figure 8. Event-triggered instants for each layer.



**Figure 9.** Time evolutions of inter-layer synchronization error  $e_p(t)$ ,  $p=1,2,\ldots,6$ : (a) ETIC-PII (4) with (30); (b) ETDIC (4) with (31).

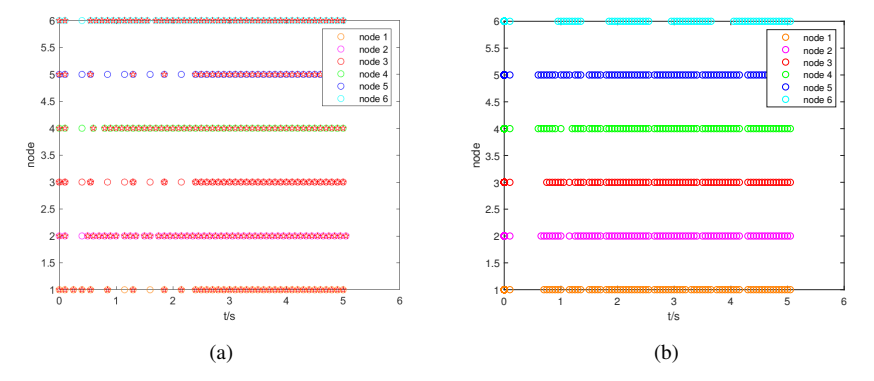


Figure 10. Event-triggered instants for each node in any layer.

the contrary, the inter-layer synchronisation of errors under ETDIC (4) and (31) does not reach the triggering condition after converging to 0. There are small fluctuations in errors, which suggests that the control effect of ETIC-PII (4) and (30) is more general.

Figures 10(a) and 10(b) demonstrate that event-triggered instants for all nodes across layers under ETDIC (4) with (31) exhibit high frequency, whereas those under ETIC-PII (4) with (30) maintain moderate spacing. This hybrid triggering strategy significantly reduces communication load and resource consumption.

#### 5 Conclusions

This study separately addresses intra-layer and inter-layer synchronization in SMLNs via the proposed ETDIC strategy. A novel auxiliary function is constructed to exclude Zeno behavior without requiring expectation solutions for stochastic perturbation terms unlike existing approaches. By integrating graph theory and stochastic analysis techniques, less conservative synchronization criteria are derived under ETDIC, advancing the current state of research. Numerical simulations validate the theoretical findings. Future work will investigate event-triggered pinning control for synchronizing stochastic multi-layer networks.

**Author contributions.** All authors (H.L., J.L., H.J., J.W., and C.H.) have equally contributed to this work for writing, reviewing, and editing. All authors have read and approved the published version of the manuscript.

#### Conflicts of interest.

**Acknowledgment.** The authors thank the anonymous reviewers for their thoughtful comments, which have contributed to improving the quality and clarity of the paper.

#### References

- 1. F. Alsaadi, Y. Luo, Y. Liu, Z. Wang, State estimation for delayed neural networks with stochastic communication protocol: The finite-time case, *Neurocomputing*, **281**:86–95, 2018, https://doi.org/10.1016/j.neucom.2017.11.067.
- 2. M. Hong, H. Yang, Y. Qi, J. Wu, Y. Sun, Synchronization of Kuramoto-oscillator networks under event-triggered impulsive control with noise perturbation, *Syst. Control Lett.*, **192**: 105884, 2024, https://doi.org/10.1016/j.sysconle.2024.105884.
- 3. B. Jiang, J. Lu, J. Lou, J. Qiu, Synchronization in an array of coupled neural networks with delayed impulses: Average impulsive delay method, *Neural Netw.*, **121**:452–460, 2020, https://doi.org/10.1016/j.neunet.2019.09.019.
- I. Korneev, I. Ramazanov, V. Semenov, A. Slepnev, T. Vadivasova, Synchronization effects in multiplex networks of chaotic maps with memristive interlayer coupling, *Commun. Nonlinear Sci. Numer. Simul.*, 135:108072, 2024, https://doi.org/10.1016/j.cnsns.2024. 108072.
- R. Kumar, S. Das, Y. Cao, Effects of infinite occurrence of hybrid impulses with quasisynchronization of parameter mismatched neural networks, *Neural Netw.*, 122:106–116, 2020, https://doi.org/10.1016/j.neunet.2019.10.007.

- Y. Lei, J. Li, A. Zhao, Robust piecewise adaptive control for an uncertainsemilinear parabolic distributed parameter systems, *Nonlinear Anal. Model. Control*, 27:234–253, 2022, https://doi.org/10.15388/namc.2022.27.25481.
- H. Li, J. Fang, X. Li, L. Rutkowski, T. Huang, Event-triggered impulsive synchronization of discrete-time coupled neural networks with stochastic perturbations and multiple delays, *Neural Netw.*, 132:447–460, 2020, https://doi.org/10.1016/j.neunet.2020. 09.012.
- X. Li, X. Yang, J. Cao, Event-triggered impulsive control for nonlinear delay systems, *Automatica*, 117:108981, 2020, https://doi.org/10.1016/j.automatica. 2020.108981.
- 9. S. Ling, H. Shi, H. Wang, P. Liu, Exponential synchronization of delayed coupled neural networks with delay-compensatory impulsive control, *ISA Trans.*, **144**:133–144, 2024, https://doi.org/10.1016/j.isatra.2023.11.015.
- H. Liu, J. Li, Z. Li, Z. Zeng, J. Lv, Intralayer synchronization of multiplex dynamical networks via pinning impulsive control, *IEEE T. Cybern.*, 52:2110–2122, 2022, https://doi.org/ 10.1109/TCYB.2020.3006032.
- M. Liu, J. Chen, H. Jiang, Z. Yu, C. Hu, B. Lu, Synchronization of chaotic delayed systems via intermittent control and its adaptive strategy, *Nonlinear Anal. Model. Control*, 26:993–1011, 2021, https://doi.org/10.15388/namc.2021.26.24419.
- 12. Q. Liu, B. Kan, Q. Wang, Y. Fang, Cluster synchronization of markovian switching complex networks with hybrid couplings and stochastic perturbations, *Physica A*, **526**:120937, 2019, https://doi.org/10.1016/j.physa.2019.04.173.
- S. Liu, L. Zhao, W. Zhang, X. Yang, F. Alsaadi, Fast fixed-time synchronization of t-s fuzzy complex networks, *Nonlinear Anal. Model. Control*, 26:597–609, 2021, https://doi. org/10.15388/namc.2021.26.23060.
- 14. D. Ning, Z. Fan, X. Wu, X. Han, Interlayer synchronization of duplex time-delay network with delayed pinning impulses, *Neurocomputing*, 452:127–136, 2021, https://doi.org/10. 1016/j.neucom.2021.04.041.
- D. Ning, X. Wu, H. Feng, Y. Chen, J. Lu, Inter-layer generalized synchronization of two-layer impulsively-coupled networks, *Commun. Nonlinear Sci. Numer. Simul.*, 79:104947, 2019, https://doi.org/10.1016/j.cnsns.2019.104947.
- J. Ren, Q. Song, Y. Gao, M. Zhao, G. Lu, Leader-following consensus of delayed neural networks under multi-layer signed graphs, *Neurocomputing*, 450:168–182, 2021, https://doi.org/10.1016/j.neucom.2021.03.009.
- Y. Ren, H. Jiang, C. Hu, X. Li, X. Qin, Discontinuous control for exponential synchronization of complex-valued stochastic multi-layer networks, *Chaos Solitons Fractals*, 174:113792, 2023, https://doi.org/10.1016/j.chaos.2023.113792.
- L. Shi, J. Li, H. Jiang, J. Wang, Quasi-synchronization of multi-layer delayed neural networks with parameter mismatches via impulsive control, *Chaos Solitons Fractals*, 175:113994, 2023, https://doi.org/10.1016/j.chaos.2023.113994.
- S. Sun, T. Ren, Y. Xu, Pinning synchronization control for stochastic multi-layer networks with coupling disturbance, *ISA Trans.*, 128:450–459, 2022, https://doi.org/10.1016/j. isatra.2021.10.016.

 S. Sun, Z. Wang, C. Jin, Y. Feng, M. Xiao, C. Zheng, Event-triggered synchronization of a two-layer heterogeneous neural network via hybrid control, *Commun. Nonlinear Sci. Numer.* Simul., 123:107279, 2023, https://doi.org/10.1016/j.cnsns.2023.107279.

- 21. M. Wang, X. Li, P. Duan, Event-triggered delayed impulsive control for nonlinear systems with application to complex neural networks, *Neural Netw.*, **150**:213–221, 2022, https://doi.org/10.1016/j.neunet.2022.03.007.
- 22. Y. Wu, S. Fu, W. Li, Exponential synchronization for coupled complex networks with time-varying delays and stochastic perturbations via impulsive control, *J. Franklin Inst.*, **356**:492–513, 2019, https://doi.org/10.1016/j.jfranklin.2018.11.003.
- 23. Y. Xu, X. Wu, B. Mao, J. Lv, C. Xie, Finite-time intra-layer and inter-layer quasi-synchronization of two-layer multi-weighted networks, *IEEE Trans. Circuits Syst. I, Regul. Pap.*, **68**:1589–1598, 2021, https://doi.org/10.1109/TCSI.2021.3050988.
- 24. N. Yang, R. Ji, H. Su, Event-triggered delayed impulsive control for synchronization of stochastic complex networks under deception attacks, *Neurocomputing*, **543**:126256, 2023, https://doi.org/10.1016/j.neucom.2023.126256.
- 25. N. Yu, W. Zhu, Exponential stabilization of fractional-order continuous-time dynamic systems via event-triggered impulsive control, *Nonlinear Anal. Model. Control*, **27**:592–608, 2022, https://doi.org/10.15388/namc.2022.27.26638.
- 26. C. Zhang, R. Li, Q. Zhu, Q. Xu, Topology identification for stochastic multi-layer networks via graph-theoretic method, *Neural Netw.*, **165**:150–163, 2023, https://doi.org/10.1016/j.neunet.2023.05.036.
- 27. C. Zhang, C. Zhang, X. Zhang, F. Wang, Y. Liang, Dynamic event-triggered control for intral inter-layer synchronization in multi-layer networks, *Commun. Nonlinear Sci. Numer. Simul.*, 119:107124, 2023, https://doi.org/10.1016/j.cnsns.2023.107124.
- R. Zhang, D. Zeng, J. Park, Y. Liu, S. Zhong, Pinning event-triggered sampling control for synchronization of t-s fuzzy complex networks with partial and discrete-time couplings, *IEEE Trans. Fuzzy Syst.*, 27:2368–2380, 2019, https://doi.org/10.1109/TFUZZ.2019. 2898373.
- T. Zhao, C. Hu, J. Yu, L. Wang, H. Jiang, Complete synchronization in fixed/preassigned time of multilayered heterogeneous networks, *ISA Trans.*, 136:254–266, 2023, https://doi. org/10.1016/j.isatra.2022.10.043.
- 30. Y. Zhou, Y. Liu, Y. Zhao, M. Cao, G. Chen, Fully distributed prescribed-time bipartite synchronization of general linear systems: An adaptive gain scheduling strategy, *Automatica*, **161**: 111459, 2024, https://doi.org/10.1016/j.automatica.2023.111459.
- 31. Y. Zhou, Z. Zeng, Event-triggered impulsive control on quasi-synchronization of memristive neural networks with time-varying delays, *Neural Netw.*, **110**:55–65, 2019, https://doi.org/10.1016/j.neunet.2018.09.014.
- 32. R. Zhu, Y. Guo, F. Wang, Quasi-synchronization of heterogeneous neural networks with distributed and proportional delays via impulsive control, *Chaos Solitons Fractals*, **141**: 110322, 2020, https://doi.org/10.1016/j.chaos.2020.110322.